

# FRASA: Feedback Retransmission Approximation for the Stability Region of Finite-User Slotted ALOHA

Ka-Hung Hui, *Student Member, IEEE*, On-Ching Yue, *Senior Member, IEEE*,  
and Wing-Cheong Lau, *Senior Member, IEEE*

**Abstract**—FRASA, *Feedback Retransmission Approximation for Slotted ALOHA*, is proposed to study the stability region of finite-user slotted ALOHA under collision channel. With FRASA, the stability region is derived in *closed form* for any number of users in the system. The result derived from FRASA is shown to be identical to the analytical result of finite-user slotted ALOHA when there are two users. It is shown that the stability region obtained from FRASA is a good *approximation* to the stability region of finite-user slotted ALOHA. The *convex hull bound*, which is convex, piecewise linear and outer-bounds the stability region of FRASA, is provided. *p-convexity*, an essential property that the stability region of FRASA should have to ensure the convex hull bound to be close to the boundary, is characterized. From these, it is derived that the stability region of FRASA can never be convex when there are more than two users. A separate convex and piecewise linear inner bound on the stability region of FRASA, the *supporting hyperplane bound*, is also given. More insights on the characterization of the capacity region of other types of wireless random access networks can be obtained from the analytical findings with FRASA.

**Index Terms**—Stability Region, Random Access, Slotted ALOHA, FRASA.

## I. INTRODUCTION

THE study of the stability region of slotted ALOHA has attracted many researchers [1]–[9]. Despite the simplicity of slotted ALOHA, this problem is extremely difficult when  $M$ , the number of users in the system, exceeds two, even on the collision channel assumption. Under this assumption, successful transmissions occur if and only if there is one active transmitter, because of the interference among the stations. The inherent difficulty in the analysis is due to the effect of queuing in each transmitter. More specifically, the probability of successful transmission depends on the number of active transmitters, which in turn depends on whether the queues in the transmitters are empty or not. However, it is still an open problem to obtain the stationary joint queue statistics in closed form.

Instead of finding the exact stability region, previous researchers have attempted to bound the stability region [1]–[3],

Manuscript received XXX YY, ZZZZ; revised XXX YY, ZZZZ. The material in this paper was presented in part at the 15th IEEE International Conference on Network Protocols, Beijing, China, October, 2007.

K.-H. Hui is with the Department of Electrical Engineering and Computer Science at Northwestern University, Evanston, IL 60208, USA (e-mail: nwhh575@northwestern.edu).

O.-C. Yue and W.-C. Lau are with the Department of Information Engineering at The Chinese University of Hong Kong, Shatin, Hong Kong (e-mail: onching@ie.cuhk.edu.hk; wclau@ie.cuhk.edu.hk).

[6], [8]. However, they did not require the bounds to be *convex* or *piecewise linear*, which are important in traffic engineering [10]. Requiring such properties reduces the traffic engineering problem into convex or linear programming, which are relatively more tractable. Therefore, we are motivated to derive convex and piecewise linear bounds on the stability region. We hope this work can serve as a basis and can be extended to consider multi-hop networks and interference models other than collision channel.

In this paper, we propose FRASA, *Feedback Retransmission Approximation for Slotted ALOHA*, as a surrogate to approximate finite-user slotted ALOHA. By considering FRASA, we make the following contributions:

- 1) We obtain in *closed form* the boundary of the stability region of FRASA under collision channel for any number of users in Section III. The results obtained from FRASA are identical to the analytical results of finite-user slotted ALOHA for  $M = 2$ .
- 2) We demonstrate by simulation in Section IV that the stability region obtained from FRASA is a good approximation to the stability region of finite-user slotted ALOHA. We also demonstrate that FRASA has a wider range of applicability than the existing bounds.
- 3) In Section V we provide a *convex hull bound*, which is convex, piecewise linear and outer-bounds the stability region of FRASA. This bound can be computed by using the transmission probability vector only. In Section VI we introduce *p-convexity*, which is essential to ensure the convex hull bound to be close to the boundary of the stability region of FRASA. The nonconvexity of the stability region of FRASA when  $M > 2$  follows from these results.
- 4) A convex and piecewise linear inner bound on the stability region of FRASA, called the *supporting hyperplane bound*, is given in Section VII.

For the rest of the paper, we present related works in Section II. In Section VIII we conclude the paper and discuss future works.

## II. RELATED WORKS

The study of the stability region of  $M$ -user infinite-buffer slotted ALOHA was initiated by [1] decades before, and is still an ongoing research. The authors in [1] obtained the exact stability region when  $M = 2$  under collision channel. [2] and

[3] used *stochastic dominance* and derived the same result as in [1] for the case of  $M = 2$ .

For general  $M$ , there were attempts to find the exact stability region, but there was only limited success. [5] established the boundary of the stability region, but it involves stationary joint queue statistics, which still do not have closed form to date. [9] obtained in closed form a partial characterization on the boundary of the stability region under *partial interference*.

Instead, many researchers focused on finding bounds on the stability region for general  $M$ . [1] obtained separate sufficient and necessary conditions for stability. [2] and [3] derived tighter bounds on the stability region by using stochastic dominance in different ways. [6] introduced *instability rank* and used it to improve the bounds on the stability region. However, the bounds in [2] and [6] are not always applicable. Also, the bounds obtained may not be piecewise linear.

With the advances in multi-user detection, researchers also studied this problem with the *multipacket reception* (MPR) model. [7] studied this problem in the infinite-user, single-buffer and symmetric MPR case. [8] considered the problem with finite users and infinite buffer. They obtained the boundary for the asymmetric MPR case with two users, and also the inner bound on the stability region for general  $M$ .

### III. THE FRASA MODEL

In slotted ALOHA, there is a queue of infinite buffer at each transmitter. Packet arrivals are assumed to be Bernoulli. When a packet arrives, it joins the end of the queue. The head-of-line packet is transmitted when the transmitter decides to transmit, and it remains at head-of-line until it is successfully transmitted. This is depicted in the upper part of Fig. 1.

Due to the complexity introduced by the queues, we propose FRASA, *Feedback Retransmission Approximation for Slotted ALOHA*, as a surrogate to approximate finite-user slotted ALOHA. In FRASA, the buffer in each transmitter can hold one packet only. Whenever there is a packet in the buffer, if the transmitter decides not to transmit the packet, or the transmitter cannot successfully transmit the packet due to collision, the packet will be removed from the buffer and put back in the buffer again after a random delay which is geometrically distributed. Therefore, the *aggregate arrival* of packets to the buffer, which includes the new arrivals and the retransmissions, is assumed to be Bernoulli or memoryless. Similar approximation was introduced by [11]. FRASA is shown in the lower part of Fig. 1.

Assume there are  $M$  links in the network, and the set of links is denoted by  $\mathcal{M} = \{n\}_{n=1}^M$ . Let  $\boldsymbol{\lambda} = (\lambda_n)_{n \in \mathcal{M}}$  and  $\mathbf{p} = (p_n)_{n \in \mathcal{M}}$  be the arrival rate vector and the transmission probability vector respectively. Define  $\bar{p}_n = 1 - p_n$  for all  $n \in \mathcal{M}$ . Let  $\chi_n$  be the aggregate arrival rate of link  $n \in \mathcal{M}$  where  $\chi_n$  is between zero and one. For each  $n \in \mathcal{M}$ , we define the mean of the random delay in the feedback loop to be  $\frac{1}{1 - \lambda_n}$ . Denote this FRASA system by  $\bar{\mathcal{S}}$ . We define the stability of the FRASA system  $\bar{\mathcal{S}}$  as follows.

*Definition 1:* The FRASA system  $\bar{\mathcal{S}}$  is *stable* if for each link  $n \in \mathcal{M}$ , the number of packets in the corresponding transmitter, *i.e.*, the packets in the single buffer plus the

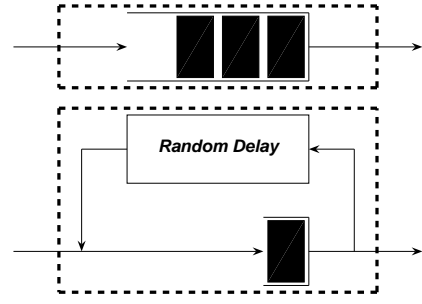


Fig. 1. Slotted ALOHA model: (Upper) Original; (Lower) FRASA.

feedback loop, does not grow to infinity. Otherwise,  $\bar{\mathcal{S}}$  is *unstable*.

Equivalently, since the number of packets in the single buffer must be finite, the stability of the feedback loop in each link determines the stability of the corresponding link in the FRASA system. Also, throughout this paper, we use the results from [12] to determine when a system is stable: on the assumption that the arrival and the service processes of a queue are stationary, the queue is stable if the average arrival rate is less than the average service rate, and the queue is unstable if the average arrival rate is larger than the average service rate.

When  $\bar{\mathcal{S}}$  is stable, for each  $n \in \mathcal{M}$ , we have

$$\chi_n = \lambda_n + \chi_n(1 - p_n) + \chi_n p_n \left[ 1 - \prod_{n' \in \mathcal{M} \setminus \{n\}} (1 - \chi_{n'} p_{n'}) \right]. \quad (1)$$

The second term on right hand side of (1) represents the arrival rate of the packets to the feedback loop due to the transmitter's decision of not transmitting the packet, while the third term on right hand side of (1) denotes the arrival rate of the packets to the feedback loop due to the transmitter's attempt to transmit the packet which results in a collision. When  $\bar{\mathcal{S}}$  is stable, the arrival rate and the departure rate of the feedback loop are equal. Therefore, together with the arrival of new packets, the three terms on right hand side of (1) constitute the aggregate arrival rate  $\chi_n$ . Simplifying (1), we get

$$\lambda_n = \chi_n p_n \prod_{n' \in \mathcal{M} \setminus \{n\}} (1 - \chi_{n'} p_{n'}), \quad (2)$$

which states that when  $\bar{\mathcal{S}}$  is stable, the loading supported by each link is equal to the successful transmission probability of the corresponding link. Since the feedback loop of each link is stable, we get for each  $n \in \mathcal{M}$

$$\chi_n(1 - p_n) + \chi_n p_n \left[ 1 - \prod_{n' \in \mathcal{M} \setminus \{n\}} (1 - \chi_{n'} p_{n'}) \right] < 1 - \lambda_n. \quad (3)$$

Substituting (2) into (3), we obtain  $\chi_n < 1$ . On the other hand, when  $\bar{\mathcal{S}}$  is unstable, the feedback loop of at least one link, say link  $n$ , is unstable. Then the departure rate of the feedback loop of link  $n$  is  $1 - \lambda_n$ . This implies that the aggregate arrival rate of link  $n$  is  $\chi_n = \lambda_n + (1 - \lambda_n) = 1$ , which means that there is

always a packet in the single buffer of the transmitter of link  $n$ . Therefore, we arrive at the following alternative definition of the stability of the FRASA system  $\bar{\mathcal{S}}$ .

*Definition 2:* The FRASA system  $\bar{\mathcal{S}}$  is *stable* if for each  $n \in \mathcal{M}$ ,  $\chi_n < 1$ . We define link  $n$  to be *infinitely backlogged* when  $\chi_n = 1$ . If  $\bar{\mathcal{S}}$  contains at least one link with infinite backlog,  $\bar{\mathcal{S}}$  is *unstable*.

To determine the stability region of FRASA, we first consider a *reduced FRASA system*. In a reduced FRASA system, we let  $M - 1$  of the links have fixed aggregate arrival rates and the remaining link is assumed with infinite backlog. Take  $\hat{n} \in \mathcal{M}$  to be the link with infinite backlog, *i.e.*,  $\chi_{\hat{n}} = 1$ , and denote this reduced FRASA system by  $\bar{\mathcal{S}}_{\hat{n}}$ . Hence, link  $\hat{n}$  is active with probability  $\chi_{\hat{n}}p_{\hat{n}} = p_{\hat{n}}$ , while for  $n \neq \hat{n}$ , link  $n$  is active with probability  $\chi_n p_n$ . Therefore,  $\bar{\lambda} = (\bar{\lambda}_n)_{n \in \mathcal{M}}$  is the successful transmission probability vector and

$$\bar{\lambda}_n = \begin{cases} \chi_n p_n (1 - p_{\hat{n}}) \prod_{n' \in \mathcal{M} \setminus \{n, \hat{n}\}} (1 - \chi_{n'} p_{n'}), & n \neq \hat{n} \\ p_{\hat{n}} \prod_{n' \in \mathcal{M} \setminus \{\hat{n}\}} (1 - \chi_{n'} p_{n'}), & n = \hat{n} \end{cases}, \quad (4)$$

with  $\bar{\lambda}_{\hat{n}} > 0$ . Then,  $\lambda_n = \bar{\lambda}_n, \forall n \in \mathcal{M}$  is the *parametric form* of the boundary of the stability region of  $\bar{\mathcal{S}}_{\hat{n}}$ . We can obtain a non-parametric version by using (4) as follows.

*Lemma 1:* Consider  $\bar{\mathcal{S}}_{\hat{n}}$ . When

$$\frac{\lambda_{\hat{n}}(1 - p_{\hat{n}})}{p_{\hat{n}}} \geq \frac{\lambda_n(1 - p_n)}{p_n} \geq 0 \quad (5)$$

is satisfied for all  $n \in \mathcal{M} \setminus \{\hat{n}\}$ , the hypersurface  $F_{\hat{n}}$ , *i.e.*,

$$\prod_{n' \in \mathcal{M}} [\lambda_{\hat{n}}(1 - p_{\hat{n}}) + \lambda_{n'} p_{\hat{n}}] = p_{\hat{n}} [\lambda_{\hat{n}}(1 - p_{\hat{n}})]^{M-1} \quad (6)$$

is the *non-parametric form* of the boundary of the stability region of  $\bar{\mathcal{S}}_{\hat{n}}$ .

*Proof:* Refer to Appendix A. ■

Recall the system is stable if all queues in the system are stable [5], [6], [8], and notice the expression  $\frac{\lambda_n(1 - p_n)}{p_n}$  in (5) is identical to the *instability rank* introduced in [6]. When  $\max_{n \in \mathcal{M}} \frac{\lambda_n(1 - p_n)}{p_n} = \frac{\lambda_{\hat{n}}(1 - p_{\hat{n}})}{p_{\hat{n}}}$  holds as in (5), link  $\hat{n}$  is the most probable one to be the first unstable link. Hence, we let link  $\hat{n}$  to be infinitely backlogged and use Lemma 1 to obtain the stability region of FRASA as in the following Theorem.

*Theorem 1:*  $\bar{\mathcal{R}} = \bigcup_{\hat{n} \in \mathcal{M}} \bar{\mathcal{R}}_{\hat{n}}$  is the stability region of

FRASA, where  $\bar{\mathcal{R}}_{\hat{n}}$  is represented by:

$$\frac{\lambda_{\hat{n}}(1 - p_{\hat{n}})}{p_{\hat{n}}} \geq \frac{\lambda_n(1 - p_n)}{p_n} \geq 0, \forall n \in \mathcal{M} \setminus \{\hat{n}\}, \quad (7)$$

$$\prod_{n' \in \mathcal{M}} [\lambda_{\hat{n}}(1 - p_{\hat{n}}) + \lambda_{n'} p_{\hat{n}}] < p_{\hat{n}} [\lambda_{\hat{n}}(1 - p_{\hat{n}})]^{M-1}. \quad (8)$$

The union here is actually a disjoint union.

*Proof:* Refer to Appendix B. ■

We first illustrate our results for  $M = 2$ . When

$$\frac{\lambda_1(1 - p_1)}{p_1} \geq \frac{\lambda_2(1 - p_2)}{p_2} \geq 0$$

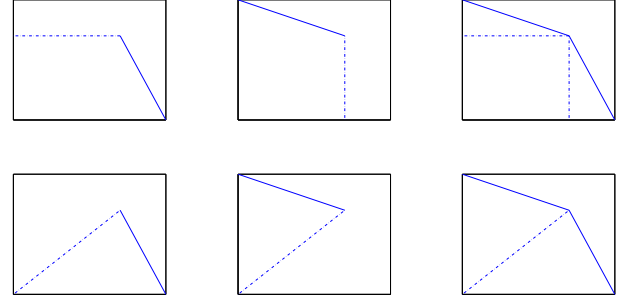


Fig. 2. Stability region with  $M = 2$ : (Upper) From [2]; (Lower) From FRASA.

holds, the boundary of the stability region of FRASA is

$$\lambda_1[\lambda_1(1 - p_1) + \lambda_2 p_1] = p_1 \lambda_1(1 - p_1),$$

which is reduced to

$$\lambda_1 = p_1 \left(1 - \frac{\lambda_2}{1 - p_1}\right)$$

after simplification. Geometrically, it is a straight line joining the points  $(p_1, 0)$  and  $(p_1 \bar{p}_2, p_2 \bar{p}_1)$ . This is depicted in the bottom left of Fig. 2. By symmetry, we also get

$$\lambda_2 = p_2 \left(1 - \frac{\lambda_1}{1 - p_2}\right)$$

as the boundary of the stability region of FRASA when

$$\frac{\lambda_2(1 - p_2)}{p_2} \geq \frac{\lambda_1(1 - p_1)}{p_1} \geq 0$$

holds. This is a straight line joining the points  $(0, p_2)$  and  $(p_1 \bar{p}_2, p_2 \bar{p}_1)$ . This is shown in the bottom center of Fig. 2. The bottom right of Fig. 2 contains the final result of the stability region obtained from FRASA. The stability region derived in [2] is illustrated in the top row of Fig. 2 for comparison. We see that the final results are identical to each other.

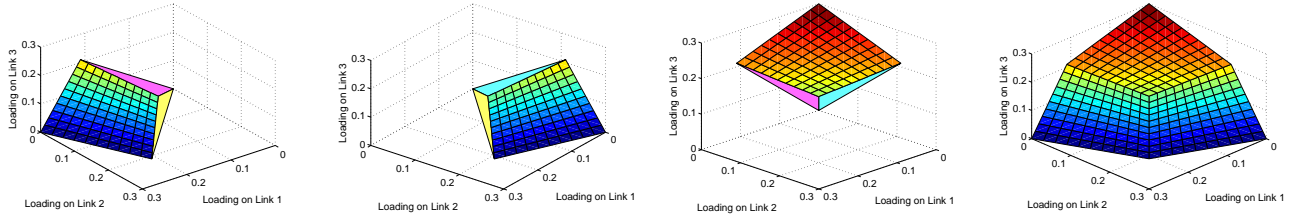
Next we consider the case of  $M = 3$  and each link has a transmission probability of 0.3. Figs. 3(a), 3(b) and 3(c) illustrate the results of Lemma 1 for  $\bar{\mathcal{S}}_1, \bar{\mathcal{S}}_2$  and  $\bar{\mathcal{S}}_3$  respectively. The single-colored hyperplanes in Figs. 3(a), 3(b) and 3(c) form the partition of the positive orthant generated by (5), while the multi-colored hypersurfaces come from (6). The union of these regions constitutes the stability region in Fig. 3(d) as stated in Theorem 1. Another example is shown in Figs. 4(a)-4(d), in which each link transmits with probability 0.6.

## IV. VALIDATION OF THE FRASA MODEL

### A. Simulation Results

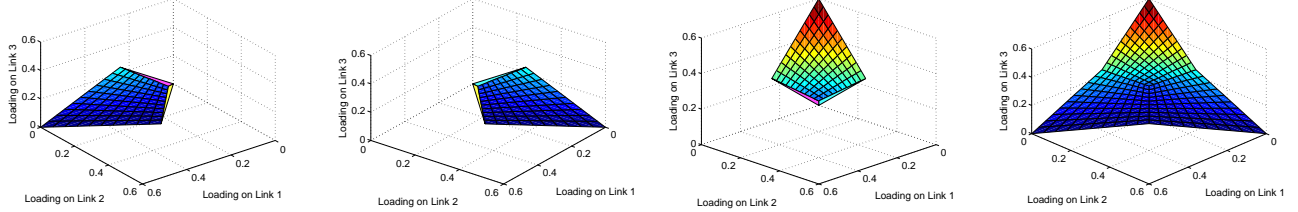
In this Section, we first use simulation to verify if FRASA is a good approximation to finite-user slotted ALOHA. Since when  $M = 2$ , we obtain identical results for both FRASA and finite-user slotted ALOHA, we consider  $M = 3$  here.

First, to check whether the slotted ALOHA system is stable or not by simulation, we extend the algorithm proposed in [13]. For each simulation run, we partition the simulation time into  $\mathcal{N}$  batches, where  $\mathcal{N} \geq 2$ . We calculate the



(a)  $\overline{\mathcal{R}}_1$ , stability region with link 1 having maximum instability rank. (b)  $\overline{\mathcal{R}}_2$ , stability region with link 2 having maximum instability rank. (c)  $\overline{\mathcal{R}}_3$ , stability region with link 3 having maximum instability rank. (d)  $\overline{\mathcal{R}}$ , the whole stability region.

Fig. 3. Stability region of FRASA with  $M = 3$  and transmission probabilities 0.3 by Lemma 1 and Theorem 1.



(a)  $\overline{\mathcal{R}}_1$ , stability region with link 1 having maximum instability rank. (b)  $\overline{\mathcal{R}}_2$ , stability region with link 2 having maximum instability rank. (c)  $\overline{\mathcal{R}}_3$ , stability region with link 3 having maximum instability rank. (d)  $\overline{\mathcal{R}}$ , the whole stability region.

Fig. 4. Stability region of FRASA with  $M = 3$  and transmission probabilities 0.6 by Lemma 1 and Theorem 1.

average queue lengths for each batch,  $\overline{Q}_{n,w}(b)$ , starting from the second batch. We discard the first batch to remove any transient behavior in the system. Then we compute the sample mean and sample variance of the average queue length, *i.e.*,  $E[\overline{Q}_{n,w}]$  and  $Var(\overline{Q}_{n,w})$ , respectively. We use the difference between the last and the second observation, *i.e.*,  $\hat{Q}_{n,w}$ , in the hypothesis testing. If,

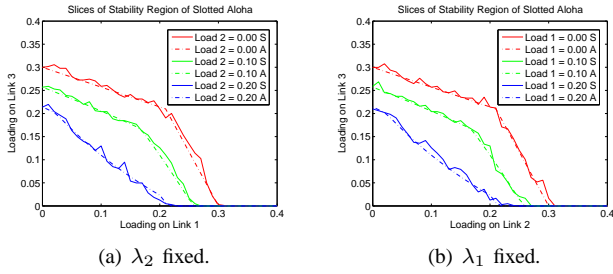
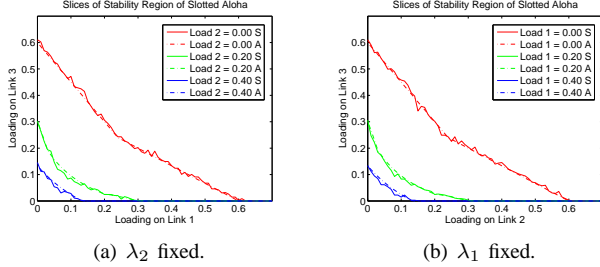
$$\frac{\hat{Q}_{n,w}}{\sqrt{2Var(\overline{Q}_{n,w})}} > t_{1-a, \mathcal{N}-2}, \exists n \in \mathcal{M}, \quad (9)$$

where  $t_{1-a, \mathcal{N}-2}$  is the  $(1-a)$ -percentile of  $t$ -distribution with  $\mathcal{N}-2$  degrees of freedom, is satisfied, we assume the system is unstable; otherwise all queues in the slotted ALOHA system is stable and so does the system. If the system is unstable, there must exist  $\hat{n} \in \mathcal{M}$  such that the length of queue  $\hat{n}$  has positive linear growth rate, making the hypothesis (9) satisfied with high probability. Otherwise, the expectation of  $\hat{Q}_{n,w}$  would be zero for all  $n \in \mathcal{M}$ , and with high probability (9) would be false. We perform  $\mathcal{W}$  simulation runs and then use majority vote to determine whether the system is stable.

Using the previous algorithm as a subroutine, we use the following approach to find the boundary of the stability region. This is based on bisection method [14]. We let  $\lambda_1$  and  $\lambda_2$  increase from zero to one. Given any  $\mathbf{p} = (p_1, p_2, p_3)$ , for any  $\lambda_1$  and  $\lambda_2$  between zero and one, let the initial search range of  $\lambda_3$  be  $[0, 1]$  and set  $\lambda_3$  to be the midpoint of the search range. Then we let  $\boldsymbol{\lambda} = (\lambda_1, \lambda_2, \lambda_3)$  be the arrival probabilities of the links and simulate the slotted ALOHA system. We use the previous algorithm to check the stability of the system. If that algorithm indicates that the system is stable, we set the next search range of  $\lambda_3$  to be the upper half of the original one; otherwise, we use the lower half as the next search range. We iterate until the search range is sufficiently small. Then we

take the midpoint of the final search range to be the boundary value of  $\lambda_3$  for the given values of  $\lambda_1$  and  $\lambda_2$ . We repeat this procedure for any combination of  $\lambda_1$  and  $\lambda_2$  to get the boundary of the stability region.

For illustrative purposes, we only show the cross-sections of the stability regions. We first let all links transmit with probability 0.3. In Fig. 5(a) we depict the cross-sections of the stability region by fixing  $\lambda_2$ , while in Fig. 5(b) the cross-sections of the stability region are obtained by fixing  $\lambda_1$ . The solid lines represent the simulation results while the dash-dot lines are obtained from FRASA. In Figs. 6(a) and 6(b) we show the corresponding results by changing the transmission probabilities of all links to 0.6. We observe that there is a close match between the stability region of FRASA and the stability region of slotted ALOHA. Slotted ALOHA and FRASA are similar in many ways. First, both define stability as the situation that the number of packets in the transmitter of each link does not grow to infinity. Second, if in every time slot, the transmission attempts of all links are the same for both slotted ALOHA and FRASA, the number of packets in the transmitter of each link are the same for both systems, except for a subtle difference: in slotted ALOHA the packets are located in the queue, while in FRASA, the packets are in the feedback loop. Also, the probability that there is a packet in the buffer are similar for both systems: when both systems are stable, the queue in slotted ALOHA and the single buffer in FRASA can be empty; on the other hand, when both systems are unstable, there is always a packet in the queue in slotted ALOHA, while the single buffer in FRASA is always occupied. Therefore, the stability region of FRASA is a good approximation to the stability region of slotted ALOHA.


 Fig. 5. Cross-section of stability region with  $M = 3$  and transmission probabilities 0.3.

 Fig. 6. Cross-section of stability region with  $M = 3$  and transmission probabilities 0.6.

### B. Comparison to Previous Bounds

Here, we demonstrate that FRASA is a good approximation to finite-user slotted ALOHA by showing the boundary values obtained from FRASA lie inside the upper and lower bounds in [6]. We fix the loading of the first  $M - 1$  links, evaluate the “FRASA” value of  $\lambda_M$ , and evaluate the “Upper” bound and “Lower” bound of  $\lambda_M$  by using Theorems 3 and 5 in [6] respectively. Before showing this, we point out that the bounds in [6] are applicable only when the instability rank assumption, *i.e.*, link  $M$  has the highest instability rank, holds. This is best illustrated by the following examples. Consider a slotted ALOHA system with two users. We let both links transmit with probability 0.6. We keep increasing  $\lambda_1$  while assuming  $\frac{\lambda_1(1-p_1)}{p_1} \leq \frac{\lambda_2(1-p_2)}{p_2}$ , and evaluate the upper bound on  $\lambda_2$  by using Theorem 3 in [6]. When  $\lambda_1 > p_1\bar{p}_2$ , the upper bound, *i.e.*,  $\lambda_{2,\max}$ , satisfies  $\frac{\lambda_2(1-p_2)}{p_2} \leq \frac{\lambda_{2,\max}(1-p_2)}{p_2} < \frac{\lambda_1(1-p_1)}{p_1}$ , showing that the instability rank assumption does not hold. We change the transmission probabilities of both links to 0.3 and repeat the whole process, but evaluate the lower bound on  $\lambda_2$  by using Theorem 5 in [6]. It is found that when  $\lambda_1 > p_1\bar{p}_2$ , the lower bound, *i.e.*,  $\lambda_{2,\min}$ , satisfies  $\frac{\lambda_{2,\min}(1-p_2)}{p_2} < \frac{\lambda_1(1-p_1)}{p_1}$ , and we cannot conclude whether the instability rank assumption is valid or not. These results are depicted in Figs. 7(a) and 7(b) respectively. In the case of  $M = 2$ , we already have the complete characterization on the boundary of the stability region, therefore we can explicitly evaluate  $\lambda_2$  and show that when  $\lambda_1 > p_1\bar{p}_2$ , the instability rank assumption does not hold, and the Theorems in [6] are not applicable. When  $M > 2$ , if there are some  $\lambda_n$  satisfying  $\lambda_n > p_n \prod_{n' \in \mathcal{M} \setminus \{n\}} \bar{p}_{n'}$ , it is difficult to predict

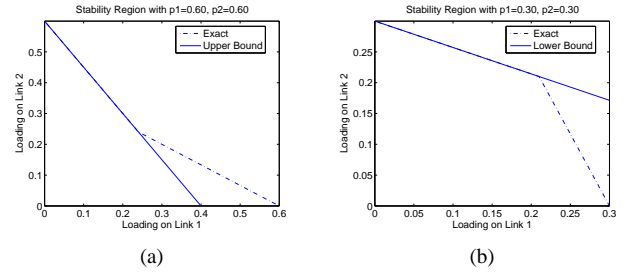


Fig. 7. Restricted application of the upper and lower bounds in [6].

whether the instability rank assumption is valid or not. When the instability rank assumption is not valid, one may tempt to switch the order of the links to keep the validity of the assumption. But in this case, we even cannot determine the stability of the links with instability ranks higher than that of link  $M$ , because the bounds on link  $n$  depend on the loadings on the links having smaller instability ranks than link  $n$  [6]. Therefore, when using the bounds in [6], we cannot set the loadings on the first  $M - 1$  links too large in order to maintain the instability rank assumption.

However, such restriction does not exist in computing the “FRASA” value of  $\lambda_M$ . We first let link  $M$  be the link with the highest instability rank, *i.e.*,  $\hat{n} = M$ . Then we solve (6) for  $\lambda_M$ , which is an equation of degree  $M - 1$ , and get  $M - 1$  values of  $\lambda_M$ . Exactly one of them is the desired value, which makes the instability rank of link  $M$  the highest. Otherwise, we find the link with the highest instability rank among the first  $M - 1$  links. We let it equals  $\hat{n}$  and solve (6) for  $\lambda_M$ , which is an equation of degree one. In this case, we get a nonnegative value which is the desired value of  $\lambda_M$ . Otherwise, we conclude that with the loadings on the first  $M - 1$  links, it is impossible to keep the system stable no matter how small  $\lambda_M$  is.

To compare the numerical values computed from FRASA against the bounds in [6], we consider the numerical examples in [2] and [6]. The examples are reproduced in Tables I–XIV. The values of the loadings are classified into four groups in each table. In G1, one or more values of  $\lambda_n$  are zero. In G2, all  $\lambda_n$  are approximately equal to  $\frac{1}{2}p_n \prod_{n' \in \mathcal{M} \setminus \{n\}} \bar{p}_{n'}$ . In G3, all  $\lambda_n$  are close to  $p_n \prod_{n' \in \mathcal{M} \setminus \{n\}} \bar{p}_{n'}$ . In G4, one or more  $\lambda_n$  satisfy  $\lambda_n > p_n \prod_{n' \in \mathcal{M} \setminus \{n\}} \bar{p}_{n'}$ , and these  $\lambda_n$  are marked with asterisks in the tables. In all cases, the values predicted from FRASA lie inside the upper and lower bounds in [6]. Simulations are also performed for all examples in [2] and [6], and the results are shown in brackets in the tables. While the difference between the simulation result and the corresponding “FRASA” value can be as large as 40% (the first case of G4 in Table II), for most cases, 82 (resp. 90) out of 96, the simulation results deviate from the corresponding “FRASA” values by at most  $\pm 2\%$  (resp.  $\pm 10\%$ ). The examples also show that the bounds in [6] may not be always applicable, as in the case of G4 in Table IV.

For the first case of G4 in Table II, we plot the contour

TABLE I  
COMPARISON FOR  $\lambda_M$  FOR  $M = 3$  AND  $p_1 = p_2 = p_3 = 0.5$ .

	$\lambda_1$	$\lambda_2$	CHB	Upper	FRASA (Sim)	Lower
G1	0	0	0.5	0.5	0.5 (0.500)	0.5
	0	0.12	0.38	0.38	0.38 (0.383)	0.38
G2	0.06	0.06	0.38	0.38	0.370 (0.365)	0.341
G3	0.12	0.123	0.257	0.257	0.170 (0.158)	0.140
G4	0.12	0.13*	0.25	0.25	0.13 (0.131)	0.13

TABLE II  
COMPARISON FOR  $\lambda_M$  FOR  $M = 3$  AND  $p_1 = 0.6, p_2 = 0.7, p_3 = 0.8$ .

	$\lambda_1$	$\lambda_2$	CHB	Upper	FRASA (Sim)	Lower
G1	0	0	0.8	0.8	0.8 (0.802)	0.8
	0	0.05	0.743	0.6	0.6 (0.601)	0.6
	0.03	0	0.76	0.68	0.68 (0.683)	0.68
G2	0.018	0.028	0.744	0.616	0.603 (0.594)	0.508
G3	0.03	0.05	0.703	0.48	0.423 (0.375)	0.24
G4	0.035	0.0561*	0.689	0.436	0.344 (0.204)	0.115
	0.025	0.0563*	0.702	0.475	0.421 (0.360)	0.278

TABLE III  
COMPARISON FOR  $\lambda_M$  FOR  $M = 3$  AND  $p_1 = 0.63, p_2 = 0.52, p_3 = 0.51$ .

	$\lambda_1$	$\lambda_2$	CHB	Upper	FRASA (Sim)	Lower
G1	0	0	0.51	0.51	0.51 (0.510)	0.51
	0	0.045	0.466	0.463	0.463 (0.464)	0.463
	0.07	0	0.453	0.437	0.437 (0.440)	0.437
G2	0.07	0.045	0.409	0.390	0.381 (0.375)	0.341
G3	0.14	0.09	0.308	0.271	0.204 (0.164)	0.123
G4	0.12	0.095*	0.320	0.286	0.233 (0.203)	0.167
	0.15*	0.093	0.297	0.257	0.166 (0.117)	0.092

TABLE IV  
COMPARISON FOR  $\lambda_M$  FOR  $M = 3$  AND  $p_1 = 0.1, p_2 = 0.1, p_3 = 0.1$ .  
(NOTE: [6]'S BOUND IS NOT APPLICABLE FOR THE EXAMPLE IN G4)

	$\lambda_1$	$\lambda_2$	CHB	Upper	FRASA (Sim)	Lower
G1	0	0	0.1	0.1	0.1 (0.100)	0.1
	0	0.03	0.097	0.097	0.097 (0.097)	0.097
G2	0.04	0.04	0.091	0.091	0.091 (0.091)	0.091
G3	0.078	0.078	0.082	0.083	0.082 (0.082)	0.082
G4	0.078	0.082*	0.076	0.082	0.076 (0.077)	0.081

TABLE V  
COMPARISON FOR  $\lambda_M$  FOR  $M = 3$  AND  $p_1 = 0.3, p_2 = 0.2, p_3 = 0.1$ .

	$\lambda_1$	$\lambda_2$	CHB	Upper	FRASA (Sim)	Lower
G1	0	0	0.1	0.1	0.1 (0.102)	0.1
	0	0.06	0.093	0.093	0.093 (0.094)	0.093
G2	0.11	0.06	0.081	0.081	0.080 (0.079)	0.079
G3	0.21	0.12	0.058	0.063	0.058 (0.057)	0.058
G4	0.11	0.13*	0.072	0.073	0.071 (0.071)	0.071

of the stability region of FRASA in Fig. 8 to investigate the reason for such a large discrepancy between the stability region of slotted ALOHA and FRASA. This contour plot shows that when  $\lambda_1$  and  $\lambda_2$  are approximately equal to 0.035 and 0.0561 respectively, the contour lines are very close together, meaning that the boundary of the stability region at  $\lambda_1 = 0.035$  and  $\lambda_2 = 0.0561$  is almost parallel to the  $\lambda_3$ -axis, i.e., the boundary is very sensitive to small changes in  $\lambda_1$  and  $\lambda_2$ . Therefore, in this situation, it is difficult to obtain the boundary of the stability region of slotted ALOHA by simulations.

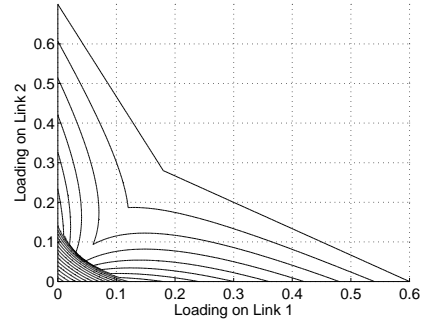


Fig. 8. Contour plot of the stability region of FRASA for the first case of G4 in Table II.

## V. CONVEX HULL BOUND

Although Theorem 1 gives us a closed-form expression for the stability region of FRASA, this stability region is not convex when  $M > 2$  (as shown in the next Section). Therefore we are motivated to derive outer and inner bounds on the stability region of FRASA that are convex and piecewise linear, which can be used to find the upper and lower bounds on network capacity respectively. In this Section, we first develop an outer bound on the stability region of FRASA that is guaranteed to be convex and piecewise linear by using *corner points* of the stability region of FRASA. For each  $\mathcal{M}' \subseteq \mathcal{M}$ , we obtain a corner point  $\Pi^{\mathcal{M}'} = \left( \Pi_n^{\mathcal{M}'} \right)_{n \in \mathcal{M}'}$ , where

$$\Pi_n^{\mathcal{M}'} = \begin{cases} p_n \prod_{n' \in \mathcal{M}' \setminus \{n\}} \bar{p}_{n'}, & n \in \mathcal{M}' \\ 0, & n \in \mathcal{M} \setminus \mathcal{M}' \end{cases}. \quad (10)$$

These corner points, by construction, lie on the boundary of the stability region of FRASA because they satisfy the parametric form (4). We first obtain the following Lemma, stating the relationship between the boundary of the stability region of FRASA and the corner points.

*Lemma 2:* The boundary of the stability region of  $\bar{\mathcal{S}}_{\hat{n}}$ , i.e., the hypersurface  $F_{\hat{n}}$ , is contained in the convex hull  $H_{\hat{n}}$  generated by the corner points  $\Pi^{\mathcal{M}' \cup \{\hat{n}\}}$  for all  $\mathcal{M}' \subseteq \mathcal{M} \setminus \{\hat{n}\}$ , i.e., every point satisfying (6) is a convex combination of the corner points  $\Pi^{\mathcal{M}' \cup \{\hat{n}\}}$  for all  $\mathcal{M}' \subseteq \mathcal{M} \setminus \{\hat{n}\}$ .

*Proof:* Refer to Appendix C. ■

By using Lemma 2 and Theorem 1, we obtain the following Theorems about using convex hulls to bound the stability region of FRASA. To obtain the bounds from these Theorems, we only have to know the coordinates of all corner points, which can be computed from (10) based on the transmission probability vector only.

*Theorem 2 (Bound of Convex-Hull Union):* The convex hull generated by  $\Pi^{\mathcal{M}' \cup \{\hat{n}\}}$  for all  $\mathcal{M}' \subseteq \mathcal{M} \setminus \{\hat{n}\}$  together with  $\mathbf{0}$ , i.e., the origin, is a piecewise linear outer bound on  $\bar{\mathcal{R}}_{\hat{n}}$ . Denote this convex hull by  $\mathcal{H}_{\hat{n}}$ . Therefore, the union of these  $\mathcal{H}_{\hat{n}}$  for all  $\hat{n} \in \mathcal{M}$ , i.e.,  $\bar{\mathcal{H}} = \bigcup_{\hat{n} \in \mathcal{M}} \mathcal{H}_{\hat{n}}$ , is a piecewise linear outer bound on the stability region of FRASA. The union here is also disjoint.

*Proof:* Refer to Appendix D. ■

TABLE VI  
COMPARISON FOR  $\lambda_M$  FOR  $M = 5$  AND  $p_1 = p_2 = p_3 = p_4 = p_5 = 0.5$ .

	$\lambda_1$	$\lambda_2$	$\lambda_3$	$\lambda_4$	CHB	Upper	FRASA (Sim)	Lower
G1	0	0	0	0	0.5	0.5	0.5 (0.500)	0.5
	0	0	0	0.015	0.485	0.485	0.485 (0.487)	0.485
	0	0	0.015	0.015	0.47	0.47	0.470 (0.469)	0.462
	0	0.015	0.015	0.015	0.455	0.455	0.453 (0.455)	0.422
G2	0.015	0.015	0.015	0.015	0.44	0.44	0.437 (0.433)	0.337
G3	0.03	0.03	0.03	0.03	0.38	0.38	0.364 (0.348)	0.048
G4	0.03	0.03	0.03	0.033*	0.377	0.377	0.360 (0.344)	0.046
	0.033*	0.032*	0.031	0.03	0.374	0.374	0.356 (0.330)	0.039
	0.0325*	0.032*	0.0315*	0.03	0.374	0.374	0.356 (0.329)	0.038

TABLE VII  
COMPARISON FOR  $\lambda_M$  FOR  $M = 5$  AND  $p_1 = 0.4, p_2 = 0.5, p_3 = 0.6, p_4 = 0.7, p_5 = 0.8$ .

	$\lambda_1$	$\lambda_2$	$\lambda_3$	$\lambda_4$	CHB	Upper	FRASA (Sim)	Lower
G1	0	0	0	0	0.8	0.8	0.8 (0.802)	0.8
	0	0	0	0.005	0.794	0.78	0.78 (0.782)	0.78
	0	0	0.005	0.005	0.788	0.76	0.759 (0.761)	0.744
	0	0.005	0.005	0.005	0.780	0.74	0.738 (0.737)	0.686
G2	0.002	0.003	0.005	0.005	0.780	0.74	0.738 (0.731)	0.629
G3	0.004	0.006	0.01	0.01	0.759	0.68	0.672 (0.664)	0.409
G4	0.004	0.006	0.01	0.017*	0.751	0.652	0.640 (0.626)	0.173
	0.004	0.006	0.011*	0.017*	0.750	0.648	0.635 (0.617)	0.152
	0.002	0.0073*	0.011*	0.017*	0.751	0.651	0.639 (0.621)	0.312

TABLE VIII  
COMPARISON FOR  $\lambda_M$  FOR  $M = 5$  AND  $p_1 = 0.77, p_2 = 0.74, p_3 = 0.63, p_4 = 0.52, p_5 = 0.51$ .

	$\lambda_1$	$\lambda_2$	$\lambda_3$	$\lambda_4$	CHB	Upper	FRASA (Sim)	Lower
G1	0	0	0	0	0.51	0.51	0.51 (0.514)	0.51
	0	0	0	0.0025	0.508	0.507	0.507 (0.507)	0.507
	0	0	0.003	0.0025	0.505	0.504	0.504 (0.508)	0.503
	0	0.007	0.003	0.0025	0.500	0.497	0.497 (0.496)	0.482
G2	0.0005	0.007	0.003	0.0025	0.500	0.496	0.496 (0.496)	0.476
G3	0.001	0.014	0.006	0.005	0.490	0.483	0.482 (0.486)	0.439
G4	0.001	0.014	0.006	0.0057*	0.489	0.482	0.482 (0.483)	0.438
	0.001	0.014	0.0089*	0.0057*	0.487	0.479	0.479 (0.477)	0.425
	0.001	0.015*	0.0089*	0.0057*	0.486	0.478	0.477 (0.479)	0.420

TABLE IX  
COMPARISON FOR  $\lambda_M$  FOR  $M = 5$  AND  $p_1 = p_2 = p_3 = p_4 = p_5 = 0.1$ .

	$\lambda_1$	$\lambda_2$	$\lambda_3$	$\lambda_4$	CHB	Upper	FRASA (Sim)	Lower
G1	0	0	0	0	0.1	0.1	0.1 (0.100)	0.1
	0	0	0	0.03	0.097	0.097	0.097 (0.097)	0.097
	0	0	0.03	0.03	0.093	0.093	0.093 (0.093)	0.093
	0	0.03	0.03	0.03	0.09	0.09	0.090 (0.091)	0.089
G2	0.03	0.03	0.03	0.03	0.863	0.087	0.086 (0.085)	0.085
G3	0.064	0.064	0.064	0.064	0.067	0.072	0.067 (0.067)	0.066
G4	0.064	0.064	0.064	0.066*	0.066	0.071	0.066 (0.067)	0.066
	0.061	0.062	0.066*	0.066*	0.067	0.072	0.067 (0.068)	0.067

*Theorem 3 (Convex Hull Bound):*  $\mathcal{H}$ , the convex hull generated by  $\Pi^{\mathcal{M}'}$  for all  $\mathcal{M}' \subseteq \mathcal{M}$ , is a convex and piecewise linear outer bound on the stability region of FRASA.

*Proof:* Refer to Appendix E. ■

In finding the bounds on  $\lambda_M$  given the loadings on the other links, we do not have to rely on the instability rank assumption as in [6]. To apply Theorem 2, we first assume link  $M$  to have the highest instability rank, and generate the corresponding convex hull. If the assumption is valid, we can find a lower bound and an upper bound from the convex hull. Otherwise, we choose from the remaining links the link with the highest instability rank and repeat the process. Theorem 3 can be applied in any case in finding the upper bound.

We demonstrate the results from these Theorems in the following examples. Figs. 9(a), 9(b) and 9(c) illustrate the results of Theorem 2, assuming the transmission probabilities of all links are 0.3. The polytopes shown in these figures are the convex hulls  $\mathcal{H}_1$ ,  $\mathcal{H}_2$  and  $\mathcal{H}_3$  generated by the corresponding corner points respectively. Fig. 9(d) shows  $\overline{\mathcal{H}}$ , the union of the convex hulls in Figs. 9(a), 9(b) and 9(c). Fig. 9(e) depicts  $\mathcal{H}$ , the convex hull generated by all corner points. The polytopes in Figs. 9(d) and 9(e) are identical. To show that this is not necessarily true, we give another example in which the transmission probabilities of all links are 0.6. In this example,  $\overline{\mathcal{H}}$  in Fig. 10(d) is contained inside  $\mathcal{H}$  in Fig. 10(e).

TABLE X  
COMPARISON FOR  $\lambda_M$  FOR  $M = 5$  AND  $p_1 = 0.05, p_2 = 0.15, p_3 = 0.2, p_4 = 0.25, p_5 = 0.3$ .

	$\lambda_1$	$\lambda_2$	$\lambda_3$	$\lambda_4$	CHB	Upper	FRASA (Sim)	Lower
G1	0	0	0	0	0.3	0.3	0.3 (0.303)	0.3
	0.008	0	0	0	0.297	0.297	0.297 (0.295)	0.297
	0.008	0.03	0	0	0.284	0.284	0.284 (0.284)	0.283
	0.008	0.03	0.04	0	0.267	0.267	0.265 (0.264)	0.263
G2	0.008	0.03	0.04	0.06	0.241	0.241	0.236 (0.236)	0.228
G3	0.015	0.05	0.08	0.1	0.175	0.195	0.171 (0.170)	0.165
G4	0.008	0.03	0.04	0.115*	0.212	0.217	0.207 (0.208)	0.202
	0.006	0.02	0.09*	0.115*	0.188	0.201	0.185 (0.183)	0.181

TABLE XI  
COMPARISON FOR  $\lambda_M$  FOR  $M = 10$  AND  $p_1 = p_2 = p_3 = p_4 = p_5 = p_6 = p_7 = p_8 = p_9 = p_{10} = 0.5$ .

	$\lambda_1$	$\lambda_2, \lambda_3$	$\lambda_4, \lambda_5$	$\lambda_6, \lambda_7, \lambda_8$	$\lambda_9$	Upper	FRASA (Sim)	Lower
G1	0	0	0	0	0	0.5	0.5 (0.500)	0.5
	0	0.00045	0.00045	0.00045	0.00045	0.496	0.496 (0.495)	0.437
G2	0.00045	0.00045	0.00045	0.00045	0.00045	0.496	0.496 (0.492)	0.362
G3	0.0009	0.0009	0.0009	0.0009	0.0009	0.492	0.492 (0.488)	0.005
G4	0.00097	0.00097	0.000977*	0.000977*	0.00098*	0.491	0.491 (0.492)	0.002
	0.00097	0.00097	0.00097	0.000977*	0.00098*	0.491	0.491 (0.492)	0.003

TABLE XII  
COMPARISON FOR  $\lambda_M$  FOR  $M = 10$  AND  $p_1 = p_2 = p_3 = 0.1, p_4 = 0.2, p_5 = 0.3, p_6 = 0.4, p_7 = 0.5, p_8 = 0.6, p_9 = 0.7, p_{10} = 0.8$ .

	$\lambda_1$ $\times 10^{-3}$	$\lambda_2, \lambda_3$ $\times 10^{-3}$	$\lambda_4$ $\times 10^{-3}$	$\lambda_5$ $\times 10^{-3}$	$\lambda_6$ $\times 10^{-3}$	$\lambda_7$ $\times 10^{-3}$	$\lambda_8$ $\times 10^{-3}$	$\lambda_9$ $\times 10^{-3}$	Upper	FRASA (Sim)	Lower
G1	0	0	0	0	0	0	0	0	0.8	0.8 (0.801)	0.8
	0	0.15	0.35	0.5	0.5	1	2	3	0.769	0.769 (0.766)	0.654
G2	0.15	0.15	0.35	0.5	0.5	1	2	3	0.769	0.768 (0.768)	0.637
G3	0.3	0.3	0.7	1	1	2	4	6	0.738	0.736 (0.735)	0.412
G4	0.3	0.3	0.7	1	1	2	4	6.86*	0.734	0.732 (0.731)	0.402
	0.01	0.327*	0.735*	1.26*	1.96*	2.94*	4.41*	6.86*	0.725	0.722 (0.719)	0.041

TABLE XIII  
COMPARISON FOR  $\lambda_M$  FOR  $M = 10$  AND  $p_1 = p_2 = p_3 = p_4 = p_5 = p_6 = p_7 = p_8 = p_9 = p_{10} = 0.1$ .

	$\lambda_1$	$\lambda_2, \lambda_3, \lambda_4$	$\lambda_5, \lambda_6, \lambda_7, \lambda_8, \lambda_9$	Upper	FRASA (Sim)	Lower
G1	0	0	0	0.1	0.1 (0.100)	0.1
	0	0.019	0.019	0.083	0.081 (0.082)	0.077
G2	0.019	0.019	0.019	0.081	0.079 (0.079)	0.073
G3	0.036	0.036	0.036	0.064	0.050 (0.050)	0.043
G4	0.039*	0.036	0.036	0.064	0.049 (0.049)	0.043
	0.039*	0.039*	0.036	0.063	0.046 (0.046)	0.041

## VI. $\mathbf{p}$ -CONVEXITY

From the examples shown in previous Section, the bounds on the stability region of FRASA obtained from Theorems 2 and 3, *i.e.*,  $\bar{\mathcal{H}}$  and  $\mathcal{H}$  respectively, need not be identical. Recall that both  $\bar{\mathcal{H}}$  and  $\mathcal{H}$  are completely characterized by the transmission probability vector only. Intuitively, for  $\bar{\mathcal{H}} = \mathcal{H}$ , we require  $\bar{\mathcal{H}}$  to be a convex set, which means the transmission probability vector may need to satisfy some ‘‘convexity’’ conditions. In this Section, we formalize these ideas and investigate the necessary and sufficient condition for  $\bar{\mathcal{H}}$  and  $\mathcal{H}$  to be identical.

We first define  $\mathbf{p}$ -convexity, and characterize the condition on the transmission probability vector for  $\mathbf{p}$ -convexity to hold.

*Definition 3:* We use the corner points  $\Pi^{\mathbf{p}^{\mathcal{M}}(\mathcal{M} \setminus \{\bar{n}\})}$  for each  $\bar{n} \in \mathcal{M}$  to form a hyperplane  $\Omega^{\mathcal{M}}$ . If the corner points  $\Pi^{\mathbf{p}^{\mathcal{M}}(\mathcal{M})}$  and  $\mathbf{0}$  lie on opposite sides of  $\Omega^{\mathcal{M}}$ , or  $\Pi^{\mathbf{p}^{\mathcal{M}}(\mathcal{M})}$  lies on  $\Omega^{\mathcal{M}}$ , the stability region of FRASA is said to be  $\mathbf{p}$ -convex.

*Theorem 4:* The stability region of FRASA is  $\mathbf{p}$ -convex if

and only if

$$\sum_{n \in \mathcal{M}} p_n \leq 1. \quad (11)$$

*Proof:* Refer to Appendix F.  $\blacksquare$

The  $\mathbf{p}$ -convexity of the stability region of FRASA can be regarded as a measure of contention level in the system.  $p_n$  can be viewed as the proportion of time that link  $n$  is active.  $\sum_{n \in \mathcal{M}} p_n \leq 1$  represents the case that the increase in channel utilization outweighs the increase in contention due to addition of one more link to the system. This is possible because when the channel utilization is small, the probability that a new link choose an idle time slot to transmit is large, therefore the contention introduced by this new link will be small and the stability region of FRASA will be  $\mathbf{p}$ -convex. On the other hand, if  $\sum_{n \in \mathcal{M}} p_n > 1$ , the contention level will be so large that it is not beneficial to introduce one more link to the system. Even in the ideal case, *i.e.*, TDMA with perfect scheduling, it is impossible to assign time slots to the links such that

TABLE XIV  
COMPARISON FOR  $\lambda_M$  FOR  $M = 10$  AND  $p_1 = p_2 = p_3 = p_4 = p_5 = 0.1, p_6 = p_7 = p_8 = p_9 = p_{10} = 0.05$ .

	$\lambda_1, \lambda_2, \lambda_3, \lambda_4, \lambda_5$	$\lambda_6$	$\lambda_7, \lambda_8$	$\lambda_9$	Upper	FRASA (Sim)	Lower
G1	0	0	0	0	0.05	0.05 (0.050)	0.05
	0	0.01	0.01	0.01	0.048	0.048 (0.048)	0.048
G2	0.025	0.01	0.01	0.01	0.041	0.040 (0.041)	0.039
G3	0.05	0.02	0.02	0.02	0.033	0.027 (0.026)	0.026
G4	0.025	0.018	0.018	0.025*	0.039	0.038 (0.037)	0.036
	0.015	0.015	0.025*	0.025*	0.041	0.040 (0.040)	0.039

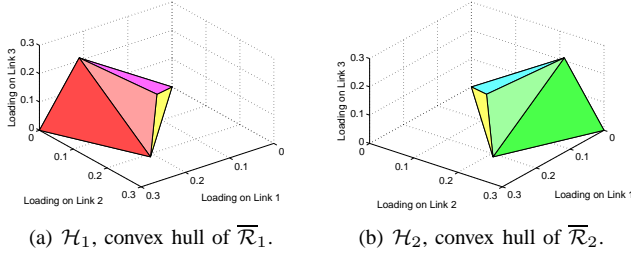


Fig. 9. Convex hull bound on the stability region of FRASA with  $M = 3$  and transmission probabilities 0.3 by Theorems 2 and 3.

there is no contention. Hence, contention is inevitable in this situation, and the stability region of FRASA will not be  $\mathbf{p}$ -convex. Consequently, it is undesirable to allow the links to be active with transmission probability vector  $(p_n)_{n \in \mathcal{M}}$ .

From (11), we observe that to make the stability region to be  $\mathbf{p}$ -convex, the transmission probabilities of all links should be set according to the number of neighboring links in proximity. For example, if we assume all links have the same priority, we may set each  $p_n$  to be  $\frac{1}{M}$ .

From Theorem 3, we know  $\overline{\mathcal{H}} \subseteq \mathcal{H}$ . We observe that if the stability region of FRASA with link set  $\mathcal{M}$  is  $\mathbf{p}$ -convex, then the stability region of FRASA with link set  $\mathcal{M}'$ , where  $\mathcal{M}' \subseteq \mathcal{M}$  and  $|\mathcal{M}'| \geq 2$ , is also  $\mathbf{p}$ -convex. It is because if (11) is satisfied, then  $\sum_{n \in \mathcal{M}'} p_n \leq 1$  must be satisfied also. We now give a necessary and sufficient condition for the equality of  $\overline{\mathcal{H}}$  and  $\mathcal{H}$  based on this observation.

*Theorem 5:*  $\overline{\mathcal{H}} = \mathcal{H}$  if and only if the stability region of

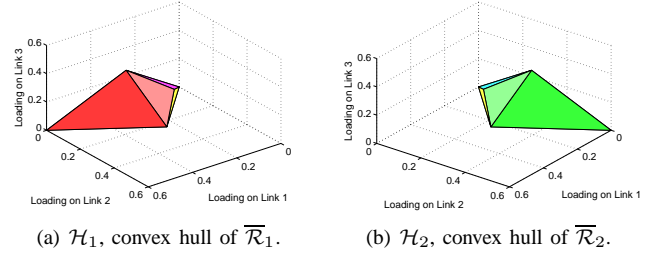


Fig. 10. Convex hull bound on the stability region of FRASA with  $M = 3$  and transmission probabilities 0.6 by Theorems 2 and 3.

FRASA is  $\mathbf{p}$ -convex.

*Proof:* Refer to Appendix G. ■

From Theorems 4 and 5, we know that (11) guarantees the stability region of FRASA to be  $\mathbf{p}$ -convex. Then, can (11) assure the convexity of the stability region of FRASA? Recall Theorem 1 that the boundary of the stability region of FRASA consists of  $M$  hypersurfaces, *i.e.*,  $F_{\hat{n}}$  for all  $\hat{n} \in \mathcal{M}$ . Also, Lemma 2 says that for each  $\hat{n} \in \mathcal{M}$ , the hypersurface  $F_{\hat{n}}$  is contained inside the convex hull  $H_{\hat{n}}$ . If (11) holds, we need an additional condition to guarantee the convexity of the stability region of FRASA: for all  $\hat{n} \in \mathcal{M}$ ,  $F_{\hat{n}}$  is a hyperplane, meaning that  $F_{\hat{n}} = H_{\hat{n}}$ . This additional condition is satisfied when  $M = 2$  as illustrated in Section III. Therefore, for  $M = 2$ ,  $\mathbf{p}$ -convexity is equivalent to convexity and (11) guarantees the convexity of the stability region of FRASA. However, this is not the case for  $M > 2$  since if such a hyperplane exists for some  $\hat{n}$ , the boundary of the stability region of FRASA is linear in  $\lambda_{\hat{n}}$ , contradicting to the non-parametric form (6) that

the boundary is of degree at least two in  $\lambda_{\hat{n}}$  when  $M > 2$ . Hence, the nonconvexity of the stability region of FRASA when  $M > 2$  follows.

Consider again the examples in Figs. 9 and 10. In Fig. 9,  $\sum_{n \in \mathcal{M}} p_n = 0.9 \leq 1$ , therefore the stability region is  $\mathbf{p}$ -convex and  $\overline{\mathcal{H}} = \mathcal{H}$ . On the other hand, in Fig. 10,  $\sum_{n \in \mathcal{M}} p_n = 1.8 > 1$ ,

and  $\overline{\mathcal{H}} \subsetneq \mathcal{H}$ . In other words, the convex hull bound is tighter if and only if the stability region is  $\mathbf{p}$ -convex. We remark that even if the stability region may not be  $\mathbf{p}$ -convex, the convex hull bound is still a valid convex and piecewise linear outer bound on the stability region of FRASA.

To illustrate the importance of  $\mathbf{p}$ -convexity, we also compute the ‘‘CHB’’ value, *i.e.*, the upper bound from Theorem 3 in Tables I-X. We observe that when the stability region of FRASA is  $\mathbf{p}$ -convex, the convex hull bound is tighter than the bound given by [6]; otherwise, the convex hull bound is looser. By Theorems 3 and 5, the convex hull bound is loose when the stability region is not  $\mathbf{p}$ -convex. This demonstrates that there is a tradeoff between the convexity and the tightness of the bounds.

## VII. SUPPORTING HYPERPLANE BOUND

In this Section, we give a convex and piecewise linear inner bound on the stability region of FRASA by using *supporting hyperplanes*. Recall that a supporting hyperplane of a convex set is a hyperplane such that it intersects with the convex set and the convex set entirely belongs to only one of the closed half spaces generated by the hyperplane. This inner bound is obtained based on the result of Lemma 2.

*Theorem 6 (Supporting Hyperplane Bound):* For each  $\hat{n} \in \mathcal{M}$ , we construct a supporting hyperplane  $P_{\hat{n}}$  which supports the convex hull  $H_{\hat{n}}$  in Lemma 2 at  $\Pi^{\mathcal{M}}(\mathcal{M})$  such that

- 1) it lies below  $H_{\hat{n}}$ ; and
- 2) it has positive intercepts on all coordinate axes.

We let  $\mathcal{S}_{\hat{n}}$  be the closed half space below  $P_{\hat{n}}$ . Then the intersection of all these half spaces in the positive orthant, *i.e.*,  $\mathcal{S} = \bigcap_{\hat{n} \in \mathcal{M}} \mathcal{S}_{\hat{n}} \cap \{\boldsymbol{\lambda}: \lambda_n \geq 0, \forall n \in \mathcal{M}\}$ , is a convex and piecewise linear inner bound on the stability region of FRASA.

*Proof:* Refer to Appendix H. ■

Consider the case that  $M = 2$  as in Fig. 11. First we choose the hyperplanes as stated in Theorem 6. Specifically, the line segment between  $(p_1, 0)$  and  $(p_1\bar{p}_2, p_2\bar{p}_1)$  is the convex hull  $H_1$ . Then we choose any point  $(p'_1, 0)$  on  $\lambda_1$ -axis such that  $p_1\bar{p}_2 \leq p'_1 \leq p_1$  and form the hyperplane  $P_1$ , *i.e.*, the line passing through  $(p'_1, 0)$  and  $(p_1\bar{p}_2, p_2\bar{p}_1)$ . Similarly, we choose a point  $(0, p'_2)$  on  $\lambda_2$ -axis such that  $p_2\bar{p}_1 \leq p'_2 \leq p_2$  and form the hyperplane  $P_2$ . These hyperplanes are shown as the red dashed lines in Fig. 11. The intersection of the closed half spaces below the red lines in the positive quadrant is the inner bound from Theorem 6.

This supporting hyperplane bound is arbitrary, in the sense that for each  $\hat{n} \in \mathcal{M}$ , as long as the hyperplane constructed satisfies the requirements listed,  $\mathcal{S}$  will be an inner bound. If

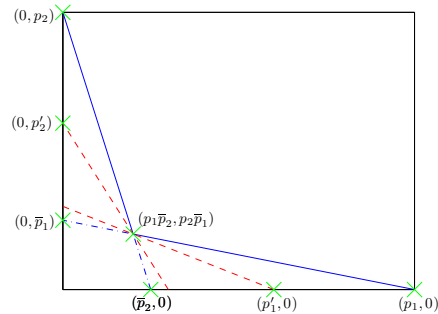


Fig. 11. Supporting hyperplane bound.

we require the inner bound to occupy the maximum hypervolume, then this problem is equivalent to finding a maximum-hypervolume convex subset of the stability region of FRASA. To the best of our knowledge, this is studied only for  $M = 2$  [15]. In this case, the problem is to find the maximum-area convex subset of a polygon. We recall some related definitions. A *reflex vertex* is a vertex of a polygon such that the angle at the vertex inside the polygon is reflex. A *chord* is a maximal line segment contained in the polygon.

First we consider the case that  $p_1 + p_2 > 1$ , *i.e.*, the stability region of FRASA is not  $\mathbf{p}$ -convex. In this case, as depicted in Fig. 11, the reflex vertex is  $(p_1\bar{p}_2, p_2\bar{p}_1)$ . By calculus, the maximum-hypervolume convex subset is either the region below the chord between  $(p_1, 0)$  and  $(0, \bar{p}_1)$ , or the region below the chord between  $(0, p_2)$  and  $(\bar{p}_2, 0)$ , depending on the values of  $p_1$  and  $p_2$ . This is a special case of the result in [15]. Suppose the region below the chord between  $(p_1, 0)$  and  $(0, \bar{p}_1)$  is the maximum-hypervolume convex subset of the stability region of FRASA. If we partition this chord about  $(p_1\bar{p}_2, p_2\bar{p}_1)$ , we obtain two line segments: one of these lies on a supporting hyperplane of the boundary between  $(p_1, 0)$  and  $(p_1\bar{p}_2, p_2\bar{p}_1)$ , while the other lies on a supporting hyperplane of the boundary between  $(0, p_2)$  and  $(p_1\bar{p}_2, p_2\bar{p}_1)$ . Similar observations can also be found when the region below the chord between  $(0, p_2)$  and  $(\bar{p}_2, 0)$  is the maximum-hypervolume convex subset of the stability region of FRASA. This means when the stability region is not  $\mathbf{p}$ -convex, if we require the inner bound to have the maximum hypervolume, the supporting hyperplanes we need in Theorem 6 coincide.

On the other hand, if the stability region of FRASA is  $\mathbf{p}$ -convex, as stated in previous Section,  $\mathbf{p}$ -convexity is equivalent to convexity. When  $p_1 + p_2 \leq 1$ , the stability region is  $\mathbf{p}$ -convex and also convex, and the stability region itself is the maximum-hypervolume convex subset. In this case, the line segments of the boundary are already the supporting hyperplanes we need.

## VIII. CONCLUSION

In this paper, we proposed FRASA, Feedback Retransmission Approximation for Slotted ALOHA, to serve as a surrogate to approximate finite-user slotted ALOHA. From FRASA, we obtained in closed form the exact stability region for any number of users in the system under collision channel.

We illustrated that the results from FRASA are identical to the analytical results of finite-user slotted ALOHA when there are two users. Simulation showed that the stability region obtained from FRASA is a good approximation to the stability region of finite-user slotted ALOHA. We demonstrated that our results from FRASA has a wider range of applicability than the existing bounds. We also established a convex hull bound, which is convex, piecewise linear and outer-bounds the stability region of FRASA. This convex hull bound can be generated by using the transmission probability vector only. We introduced  $\mathbf{p}$ -convexity, which is essential to ensure the convex hull bound to be close to the boundary of the stability region of FRASA. From these results, we deduced that the stability region of FRASA is nonconvex when there are more than two users. A separate convex and piecewise linear inner bound, supporting hyperplane bound, was also introduced.

#### APPENDIX A PROOF OF LEMMA 1

Starting from the parametric form (4), for  $n \in \mathcal{M} \setminus \{\hat{n}\}$ ,

$$\begin{aligned} \frac{\lambda_n}{\lambda_{\hat{n}}} &= \frac{\chi_n p_n (1 - p_{\hat{n}}) \prod_{n' \in \mathcal{M} \setminus \{n, \hat{n}\}} (1 - \chi_{n'} p_{n'})}{p_{\hat{n}} \prod_{n' \in \mathcal{M} \setminus \{\hat{n}\}} (1 - \chi_{n'} p_{n'})} \\ &= \frac{\chi_n p_n (1 - p_{\hat{n}})}{p_{\hat{n}} (1 - \chi_n p_n)} \end{aligned}$$

Therefore,

$$\chi_n = \frac{\lambda_n p_{\hat{n}}}{\lambda_{\hat{n}} (1 - p_{\hat{n}}) p_n + \lambda_n p_{\hat{n}} p_n}$$

and the condition  $0 \leq \chi_n \leq 1$  is translated into

$$\frac{\lambda_{\hat{n}} (1 - p_{\hat{n}})}{p_{\hat{n}}} \geq \frac{\lambda_n (1 - p_n)}{p_n} \geq 0.$$

Combining these results,

$$\begin{aligned} \lambda_{\hat{n}} &= p_{\hat{n}} \prod_{n' \in \mathcal{M} \setminus \{\hat{n}\}} (1 - \chi_{n'} p_{n'}) \\ &= p_{\hat{n}} \prod_{n' \in \mathcal{M} \setminus \{\hat{n}\}} \left[ 1 - \frac{\lambda_{n'} p_{\hat{n}} p_{n'}}{\lambda_{\hat{n}} (1 - p_{\hat{n}}) p_{n'} + \lambda_{n'} p_{\hat{n}} p_{n'}} \right] \\ &= p_{\hat{n}} \prod_{n' \in \mathcal{M} \setminus \{\hat{n}\}} \frac{\lambda_{\hat{n}} (1 - p_{\hat{n}})}{\lambda_{\hat{n}} (1 - p_{\hat{n}}) + \lambda_{n'} p_{\hat{n}}}, \end{aligned}$$

we obtain

$$\prod_{n' \in \mathcal{M}} [\lambda_{\hat{n}} (1 - p_{\hat{n}}) + \lambda_{n'} p_{\hat{n}}] = p_{\hat{n}} [\lambda_{\hat{n}} (1 - p_{\hat{n}})]^{M-1}$$

as the boundary of the stability region of  $\bar{\mathcal{S}}_{\hat{n}}$ . ■

#### APPENDIX B PROOF OF THEOREM 1

By (7), the positive orthant is partitioned into  $M$  regions. In the region that  $\max_{n \in \mathcal{M}} \frac{\lambda_n (1 - p_n)}{p_n} = \frac{\lambda_{\hat{n}} (1 - p_{\hat{n}})}{p_{\hat{n}}}$ , link  $\hat{n}$  is the most probable one to be the first link to become unstable, therefore we let link  $\hat{n}$  be the only link with infinite backlog

(in case there are more than one  $n$  that maximize the instability rank, choose one of them to be  $\hat{n}$  arbitrarily). Then from Lemma 1,

$$\prod_{n' \in \mathcal{M}} [\lambda_{\hat{n}} (1 - p_{\hat{n}}) + \lambda_{n'} p_{\hat{n}}] = p_{\hat{n}} [\lambda_{\hat{n}} (1 - p_{\hat{n}})]^{M-1}$$

is the boundary of the stability region of FRASA. Consider a point  $\boldsymbol{\lambda} = (\lambda_n)_{n \in \mathcal{M}}$  in  $M$ -dimensional space where  $\lambda_{\hat{n}} < p_{\hat{n}}$  and  $\lambda_n = 0, \forall n \in \mathcal{M} \setminus \{\hat{n}\}$ . This point lies inside the stability region of FRASA. Substituting into the above equation, we get  $\lambda_{\hat{n}} [\lambda_{\hat{n}} (1 - p_{\hat{n}})]^{M-1}$  on LHS and  $p_{\hat{n}} [\lambda_{\hat{n}} (1 - p_{\hat{n}})]^{M-1}$  on RHS. Therefore, when (7) holds,

$$\prod_{n' \in \mathcal{M}} [\lambda_{\hat{n}} (1 - p_{\hat{n}}) + \lambda_{n'} p_{\hat{n}}] < p_{\hat{n}} [\lambda_{\hat{n}} (1 - p_{\hat{n}})]^{M-1}$$

is the condition for the reduced FRASA system  $\bar{\mathcal{S}}_{\hat{n}}$  to be stable. Thus, the region formed by (7) and (8) is part of the stability region of  $\bar{\mathcal{S}}$ . By taking the union over all possible values of  $\hat{n}$ , we obtain the stability region of FRASA. ■

#### APPENDIX C PROOF OF LEMMA 2

Let  $\Pi = (\Pi_n)_{n \in \mathcal{M}}$  be a point satisfying (6). Then, from the parametric form (4),

$$\Pi_n = \begin{cases} \chi_n p_n (1 - p_{\hat{n}}) \prod_{n' \in \mathcal{M} \setminus \{n, \hat{n}\}} (1 - \chi_{n'} p_{n'}), & n \neq \hat{n} \\ p_{\hat{n}} \prod_{n' \in \mathcal{M} \setminus \{\hat{n}\}} (1 - \chi_{n'} p_{n'}), & n = \hat{n} \end{cases} \quad (12)$$

If  $\Pi$  is a convex combination of  $\Pi^{\mathcal{M}' \cup \{\hat{n}\}}$  for all  $\mathcal{M}' \subseteq \mathcal{M} \setminus \{\hat{n}\}$ , then

$$\Pi_n = \begin{cases} p_n \bar{p}_{\hat{n}} \sum_{\mathcal{M}' : n \in \mathcal{M}' \subseteq \mathcal{M} \setminus \{\hat{n}\}} \phi_{\mathcal{M}'} \prod_{n' \in \mathcal{M}' \setminus \{n\}} \bar{p}_{n'}, & n \neq \hat{n} \\ p_{\hat{n}} \sum_{\mathcal{M}' \subseteq \mathcal{M} \setminus \{\hat{n}\}} \phi_{\mathcal{M}'} \prod_{n' \in \mathcal{M}'} \bar{p}_{n'}, & n = \hat{n} \end{cases} \quad (13)$$

where

$$\sum_{\mathcal{M}' \subseteq \mathcal{M} \setminus \{\hat{n}\}} \phi_{\mathcal{M}'} = 1 \text{ and } \phi_{\mathcal{M}'} \geq 0, \forall \mathcal{M}' \subseteq \mathcal{M} \setminus \{\hat{n}\}.$$

We will show that  $\{\phi_{\mathcal{M}'}\}_{\mathcal{M}' \subseteq \mathcal{M} \setminus \{\hat{n}\}}$  always exists. When  $n = \hat{n}$ , we get

$$\sum_{\mathcal{M}' \subseteq \mathcal{M} \setminus \{\hat{n}\}} \phi_{\mathcal{M}'} \prod_{n' \in \mathcal{M}'} \bar{p}_{n'} = \prod_{n' \in \mathcal{M} \setminus \{\hat{n}\}} (1 - \chi_{n'} p_{n'}).$$

Consider this as a multinomial in  $\{p_n\}_{n \in \mathcal{M} \setminus \{\hat{n}\}}$ . By equating the coefficient of  $\prod_{n' \in \mathcal{M}''} p_{n'}$  for all  $\mathcal{M}'' \subseteq \mathcal{M} \setminus \{\hat{n}\}$ , we get

$$\sum_{\mathcal{M}'' : \mathcal{M}'' \subseteq \mathcal{M}' \subseteq \mathcal{M} \setminus \{\hat{n}\}} \phi_{\mathcal{M}''} = \prod_{n' \in \mathcal{M}''} \chi_{n'}. \quad (14)$$

Also by equating the coefficient of  $\prod_{n' \in \mathcal{M}''} p_{n'}$  for all  $\mathcal{M}'' \subseteq \mathcal{M} \setminus \{n, \hat{n}\}$  with  $n \neq \hat{n}$ , we get

$$\sum_{\mathcal{M}'' : \mathcal{M}'' \cup \{n\} \subseteq \mathcal{M}' \subseteq \mathcal{M} \setminus \{\hat{n}\}} \phi_{\mathcal{M}''} = \chi_n \prod_{n' \in \mathcal{M}''} \chi_{n'}.$$

Observe that this is only a special case of (14), it suffices to consider (14) only. Notice that (14) is a system of linear equations. By Gaussian elimination, we see that for all  $\mathcal{M}'' \subseteq \mathcal{M} \setminus \{\hat{n}\}$ ,

$$\begin{aligned} \phi_{\mathcal{M}''} &= \sum_{\mathcal{M}': \mathcal{M}'' \subseteq \mathcal{M}' \subseteq \mathcal{M} \setminus \{\hat{n}\}} (-1)^{|\mathcal{M}'| - |\mathcal{M}''|} \prod_{n' \in \mathcal{M}''} \chi_{n'} \\ &= \prod_{n' \in \mathcal{M}''} \chi_{n'} \prod_{n'' \in \mathcal{M} \setminus (\mathcal{M}'' \cup \{\hat{n}\})} (1 - \chi_{n''}) \geq 0. \end{aligned}$$

Also, by considering  $\mathcal{M}'' = \emptyset$  in (14), we obtain

$$\sum_{\mathcal{M}' \subseteq \mathcal{M} \setminus \{\hat{n}\}} \phi_{\mathcal{M}'} = 1.$$

Therefore, every point satisfying (6) is a convex combination of  $\Pi^{\mathcal{M}(\mathcal{M}' \cup \{\hat{n}\})}$  for all  $\mathcal{M}' \subseteq \mathcal{M} \setminus \{\hat{n}\}$ . ■

#### APPENDIX D PROOF OF THEOREM 2

Consider the reduced FRASA system  $\bar{\mathcal{S}}_{\hat{n}}$  and let  $\mathcal{M}' \subseteq \mathcal{M} \setminus \{\hat{n}\}$ . From (10), for every  $n \in \mathcal{M} \setminus \{\hat{n}\}$ , all corner points  $\Pi^{\mathcal{M}(\mathcal{M}' \cup \{\hat{n}\})}$  with  $n \in \mathcal{M}'$  and  $\mathbf{0}$  lie on the boundary  $\frac{\lambda_{\hat{n}}(1 - p_{\hat{n}})}{p_{\hat{n}}} = \frac{\lambda_n(1 - p_n)}{p_n}$ , all corner points  $\Pi^{\mathcal{M}(\mathcal{M}' \cup \{\hat{n}\})}$  with  $n \notin \mathcal{M}' \cup \{\hat{n}\}$  and  $\mathbf{0}$  lie on the boundary  $\frac{\lambda_n(1 - p_n)}{p_n} = 0$ . Also, for all  $n \in \mathcal{M} \setminus \{\hat{n}\}$ , the condition  $0 \leq \chi_n \leq 1$  implies none of the corner points lie outside the region  $\frac{\lambda_{\hat{n}}(1 - p_{\hat{n}})}{p_{\hat{n}}} \geq \frac{\lambda_n(1 - p_n)}{p_n} \geq 0$ . Hence, for all  $n \in \mathcal{M} \setminus \{\hat{n}\}$ ,  $\frac{\lambda_{\hat{n}}(1 - p_{\hat{n}})}{p_{\hat{n}}} = \frac{\lambda_n(1 - p_n)}{p_n}$  and  $\frac{\lambda_n(1 - p_n)}{p_n} = 0$  are the boundaries of both  $\bar{\mathcal{R}}_{\hat{n}}$  and  $\mathcal{H}_{\hat{n}}$ . Therefore, from Lemma 2,  $\bar{\mathcal{R}}_{\hat{n}} \subseteq \mathcal{H}_{\hat{n}}$ , and  $\bar{\mathcal{R}} = \bigcup_{\hat{n} \in \mathcal{M}} \bar{\mathcal{R}}_{\hat{n}} \subseteq \bigcup_{\hat{n} \in \mathcal{M}} \mathcal{H}_{\hat{n}} = \bar{\mathcal{H}}$ . Since the boundaries  $\frac{\lambda_{\hat{n}}(1 - p_{\hat{n}})}{p_{\hat{n}}} = \frac{\lambda_n(1 - p_n)}{p_n}$  and  $\frac{\lambda_n(1 - p_n)}{p_n} = 0$  are linear and the convex hull generated by a set of points is piecewise linear,  $\bar{\mathcal{H}}$  is piecewise linear. ■

#### APPENDIX E PROOF OF THEOREM 3

Notice that  $\mathcal{H}$  is the convex hull of  $\bar{\mathcal{H}}$ . Since the union of convex sets need not be convex, it is trivial to see that  $\bar{\mathcal{H}} \subseteq \mathcal{H}$ . Therefore from Theorem 2,  $\bar{\mathcal{R}} \subseteq \mathcal{H}$ . By the same reason as in proving Theorem 2,  $\mathcal{H}$  is also piecewise linear. ■

#### APPENDIX F PROOF OF THEOREM 4

Introduce the following notations:

$$\begin{aligned} p_{(x,y)}^{\mathcal{M}} &= \prod_{n' \in \mathcal{M} \setminus \{x,y\}} \bar{p}_{n'}, \\ p_{(x)}^{\mathcal{M}} &= \prod_{n' \in \mathcal{M} \setminus \{x\}} \bar{p}_{n'}. \end{aligned}$$

Then, for each  $\bar{n} \in \mathcal{M}$ ,  $\Pi^{\mathcal{M}(\mathcal{M} \setminus \{\bar{n}\})} = \left( \Pi_n^{\mathcal{M}(\mathcal{M} \setminus \{\bar{n}\})} \right)_{n \in \mathcal{M}}$  is a point in  $M$ -dimensional space with

$$\Pi_n^{\mathcal{M}(\mathcal{M} \setminus \{\bar{n}\})} = \begin{cases} p_n p_{(n,\bar{n})}^{\mathcal{M}}, & n \neq \bar{n} \\ 0, & n = \bar{n} \end{cases},$$

and  $\Pi^{\mathcal{M}(\mathcal{M})} = \left( \Pi_n^{\mathcal{M}(\mathcal{M})} \right)_{n \in \mathcal{M}}$  is another point with

$$\Pi_n^{\mathcal{M}(\mathcal{M})} = p_n p_{(n)}^{\mathcal{M}}, \forall n \in \mathcal{M}.$$

To determine whether the stability region of FRASA is  $\mathbf{p}$ -convex, we need the following two Lemmas.

*Lemma 3:* Let  $\mathcal{X}_{\mathcal{M}}$  be a  $M \times M$  matrix, with the first row equals  $\mathbf{0} - \Pi^{\mathcal{M}(\mathcal{M} \setminus \{1\})}$ , and for  $n \in \mathcal{M} \setminus \{1\}$ , the  $n$ -th row is  $\Pi^{\mathcal{M}(\mathcal{M} \setminus \{n\})} - \Pi^{\mathcal{M}(\mathcal{M} \setminus \{1\})}$ . Then

$$|\mathcal{X}_{\mathcal{M}}| = (-1)^M (M-1) \prod_{n' \in \mathcal{M}} p_{n'} \prod_{n'' \in \mathcal{M}} \bar{p}_{n''}^{M-2}. \quad (15)$$

*Lemma 4:* Let  $\mathcal{Y}_{\mathcal{M}}$  be a  $M \times M$  matrix, with the first row equals  $\Pi^{\mathcal{M}(\mathcal{M})} - \Pi^{\mathcal{M}(\mathcal{M} \setminus \{1\})}$ , and for  $n \in \mathcal{M} \setminus \{1\}$ , the  $n$ -th row is  $\Pi^{\mathcal{M}(\mathcal{M} \setminus \{n\})} - \Pi^{\mathcal{M}(\mathcal{M} \setminus \{1\})}$ . Then

$$|\mathcal{Y}_{\mathcal{M}}| = (-1)^M \left( \sum_{n \in \mathcal{M}} p_n - 1 \right) \prod_{n' \in \mathcal{M}} p_{n'} \prod_{n'' \in \mathcal{M}} \bar{p}_{n''}^{M-2}. \quad (16)$$

$|\mathcal{X}_{\mathcal{M}}|$  is calculated as follows:

$$\begin{aligned} |\mathcal{X}_{\mathcal{M}}| &= - \begin{vmatrix} 0 & p_2 p_{(2,1)}^{\mathcal{M}} & \cdots & p_M p_{(M,1)}^{\mathcal{M}} \\ p_1 p_{(1,2)}^{\mathcal{M}} & 0 & \cdots & p_M p_{(M,2)}^{\mathcal{M}} \\ \vdots & \vdots & \ddots & \vdots \\ p_1 p_{(1,M)}^{\mathcal{M}} & p_2 p_{(2,M)}^{\mathcal{M}} & \cdots & 0 \end{vmatrix} \\ &= - \prod_{n' \in \mathcal{M}} p_{n'} \prod_{n'' \in \mathcal{M}} \bar{p}_{n''}^{M-2} \begin{vmatrix} 0 & 1 & \cdots & 1 \\ 1 & 0 & \cdots & 1 \\ \vdots & \vdots & \ddots & \vdots \\ 1 & 1 & \cdots & 0 \end{vmatrix} \\ &= (-1)^M (M-1) \prod_{n' \in \mathcal{M}} p_{n'} \prod_{n'' \in \mathcal{M}} \bar{p}_{n''}^{M-2} \end{aligned}$$

The first equality is obtained by subtracting the first row of  $\mathcal{X}_{\mathcal{M}}$  from all other rows in  $\mathcal{X}_{\mathcal{M}}$ . The second equality results from the observation that if for all  $n'' \in \mathcal{M}$  we multiply  $\bar{p}_{n''}$  to both the  $n''$ -th row and column, then we have a factor of  $\prod_{n'' \in \mathcal{M}} \bar{p}_{n''}$  from each element in  $\mathcal{X}_{\mathcal{M}}$ .  $|\mathcal{Y}_{\mathcal{M}}|$  is obtained similarly as shown below:

$$\begin{aligned} |\mathcal{Y}_{\mathcal{M}}| &= - \begin{vmatrix} -p_1 p_{(1)}^{\mathcal{M}} & p_1 p_2 p_{(2,1)}^{\mathcal{M}} & \cdots & p_1 p_M p_{(M,1)}^{\mathcal{M}} \\ p_2 p_1 p_{(1,2)}^{\mathcal{M}} & -p_2 p_{(2)}^{\mathcal{M}} & \cdots & p_2 p_M p_{(M,2)}^{\mathcal{M}} \\ \vdots & \vdots & \ddots & \vdots \\ p_M p_1 p_{(1,M)}^{\mathcal{M}} & p_M p_2 p_{(2,M)}^{\mathcal{M}} & \cdots & -p_M p_{(M)}^{\mathcal{M}} \end{vmatrix} \\ &= - \prod_{n' \in \mathcal{M}} p_{n'} \prod_{n'' \in \mathcal{M}} \bar{p}_{n''}^{M-2} \begin{vmatrix} -\bar{p}_1 & p_1 & \cdots & p_1 \\ p_2 & -\bar{p}_2 & \cdots & p_2 \\ \vdots & \vdots & \ddots & \vdots \\ p_M & p_M & \cdots & -\bar{p}_M \end{vmatrix} \\ &= (-1)^M \left( \sum_{n \in \mathcal{M}} p_n - 1 \right) \prod_{n' \in \mathcal{M}} p_{n'} \prod_{n'' \in \mathcal{M}} \bar{p}_{n''}^{M-2} \end{aligned}$$

The proof of Theorem 4 goes as follows. We first construct a normal vector perpendicular to the hyperplane  $\Omega^{\mathcal{M}}$ . If we let  $\{\mathbf{e}_n\}_{n \in \mathcal{M}}$  be the set of basis vector where  $\mathbf{e}_n$  is a unit vector in the direction of increasing  $\lambda_n$ , then

$$\mathbf{n} = \begin{pmatrix} \mathbf{e}_1 & \mathbf{e}_2 & \cdots & \mathbf{e}_n \\ N_1^2 & N_2^2 & \cdots & N_M^2 \\ \vdots & \vdots & \ddots & \vdots \\ N_1^M & N_2^M & \cdots & N_M^M \end{pmatrix}$$

with

$$N_n^{\bar{n}} = \Pi_n^{\mathcal{M}(\mathcal{M} \setminus \{\bar{n}\})} - \Pi_n^{\mathcal{M}(\mathcal{M} \setminus \{1\})}$$

will be a normal vector of  $\Omega^{\mathcal{M}}$ . Therefore,  $|\mathcal{X}_{\mathcal{M}}|$  is the inner product of  $\mathbf{0} - \Pi_n^{\mathcal{M}(\mathcal{M} \setminus \{1\})}$  and  $\mathbf{n}$ , while  $|\mathcal{Y}_{\mathcal{M}}|$  is the inner product of  $\Pi_n^{\mathcal{M}(\mathcal{M})} - \Pi_n^{\mathcal{M}(\mathcal{M} \setminus \{1\})}$  and  $\mathbf{n}$ .  $\Pi_n^{\mathcal{M}(\mathcal{M})}$  lies on  $\Omega^{\mathcal{M}}$  is equivalent to  $|\mathcal{Y}_{\mathcal{M}}| = 0$ .  $\Pi_n^{\mathcal{M}(\mathcal{M})}$  and  $\mathbf{0}$  lie on opposite sides of  $\Omega^{\mathcal{M}}$  is equivalent to that  $|\mathcal{X}_{\mathcal{M}}|$  and  $|\mathcal{Y}_{\mathcal{M}}|$  have opposite signs. With the condition that  $\mathbf{0}$  never lies on  $\Omega^{\mathcal{M}}$ ,  $\mathbf{p}$ -convexity is achieved if and only if  $|\mathcal{X}_{\mathcal{M}}| |\mathcal{Y}_{\mathcal{M}}| \leq 0$ . From Lemmas 3 and 4, the condition is equivalent to

$$(-1)^{2M} (M-1) \left( \sum_{n \in \mathcal{M}} p_n - 1 \right) \prod_{n' \in \mathcal{M}} p_{n'}^2 \prod_{n'' \in \mathcal{M}} \bar{p}_{n''}^{2(M-2)} \leq 0.$$

After simplification, it reduces to (11). ■

## APPENDIX G PROOF OF THEOREM 5

Notice that  $\mathcal{H}$  is the convex hull of  $\bar{\mathcal{H}}$ . The corner points either lie on the boundary of  $\mathcal{H}$  or in the interior of  $\mathcal{H}$ . If the stability region of FRASA is  $\mathbf{p}$ -convex, we only need to show that all corner points lie on the boundary of  $\mathcal{H}$ . It is because if all corner points are on the boundary of  $\mathcal{H}$ , then the union  $\bigcup_{\hat{n} \in \mathcal{M}} \mathcal{H}_{\hat{n}}$  is convex and hence  $\bar{\mathcal{H}} = \mathcal{H}$ . Consider

$M = 2$ . When forming the convex hull  $\mathcal{H}$ , either

- 1)  $\Pi_n^{\mathcal{M}(\mathcal{M})}$  lies on  $\Omega^{\mathcal{M}}$ , meaning that  $\Omega^{\mathcal{M}}$  is part of the boundary of  $\mathcal{H}$ ; or
- 2)  $\Pi_n^{\mathcal{M}(\mathcal{M})}$  and  $\mathbf{0}$  lie on opposite sides of  $\Omega^{\mathcal{M}}$ , which means  $\Omega^{\mathcal{M}}$  will not be the boundary of  $\mathcal{H}$  because there is a corner point  $\Pi_n^{\mathcal{M}(\mathcal{M})}$  lying beyond  $\Omega^{\mathcal{M}}$ .

In both cases,  $\Pi_n^{\mathcal{M}(\mathcal{M})}$  lies on the boundary of  $\mathcal{H}$ . For general values of  $M$  greater than two, we consider all  $\mathcal{M}' \subseteq \mathcal{M}$  where  $2 \leq |\mathcal{M}'| < M$  in ascending order of  $|\mathcal{M}'|$ . Because the stability region of FRASA with link set  $\mathcal{M}'$  is also  $\mathbf{p}$ -convex, by repeating the arguments as above, we see that now all corner points except  $\Pi_n^{\mathcal{M}(\mathcal{M})}$  are on the boundary of  $\mathcal{H}$  and  $\Omega^{\mathcal{M}}$  is the boundary of the stability region farthest away from  $\mathbf{0}$ . Now we consider the corner point  $\Pi_n^{\mathcal{M}(\mathcal{M})}$ . We can apply similar arguments as above to show that  $\Pi_n^{\mathcal{M}(\mathcal{M})}$  lies on the boundary of  $\mathcal{H}$ . Hence,  $\bar{\mathcal{H}} = \mathcal{H}$ . On the other hand, if the stability region of FRASA is not  $\mathbf{p}$ -convex, then  $\Pi_n^{\mathcal{M}(\mathcal{M})}$  lies in between  $\mathbf{0}$  and  $\Omega^{\mathcal{M}}$ . Therefore, at least one corner point does not lie on the boundary of  $\mathcal{H}$  and  $\bar{\mathcal{H}} \subsetneq \mathcal{H}$ . ■

## APPENDIX H PROOF OF THEOREM 6

Consider the bound of convex hull union  $\bar{\mathcal{H}}$  in Theorem 2. Choose an arbitrary  $\hat{n} \in \mathcal{M}$ . When  $\bar{\mathcal{H}}$  is intersected with the closed half space  $\mathcal{S}_{\hat{n}}$ , the resultant polytope does not contain the convex hull  $\mathcal{H}_{\hat{n}}$  by construction. Therefore, this resultant polytope excludes the hypersurface  $\mathcal{F}_{\hat{n}}$ . We repeat this argument for all  $\hat{n} \in \mathcal{M}$ , then for all  $\hat{n} \in \mathcal{M}$ , the convex hull  $\mathcal{H}_{\hat{n}}$  together with the hypersurface  $\mathcal{F}_{\hat{n}}$  are removed. The boundary of the resultant polytope is consisted of  $\mathcal{P}_{\hat{n}}$  for all  $\hat{n} \in \mathcal{M}$  and the boundary of the positive orthant only, and hence the polytope is  $\mathcal{S}$ . Therefore,  $\mathcal{S}$  is a subset of  $\bar{\mathcal{R}}$  and constitutes an inner bound on the stability region of FRASA. This bound is convex and piecewise linear since half spaces are convex and piecewise linear, and these two properties are preserved under intersection. ■

## REFERENCES

- [1] B. S. Tsybakov and V. A. Mikhailov, "Ergodicity of a Slotted ALOHA System," *Probl. Inform. Transm.*, vol. 15, no. 4, pp. 73–87, 1979.
- [2] R. R. Rao and A. Ephremides, "On the Stability of Interacting Queues in a Multiple-Access System," *IEEE Trans. Inf. Theory*, vol. 34, no. 5, pp. 918–930, Sep. 1988.
- [3] W. Szpankowski, "Stability Conditions for Multidimensional Queueing Systems with Computer Applications," *Oper. Res.*, vol. 36, no. 6, pp. 944–957, Nov./Dec. 1988.
- [4] V. Anantharam, "The Stability Region of the Finite-User Slotted ALOHA Protocol," *IEEE Trans. Inf. Theory*, vol. 37, no. 3, pp. 535–540, May 1991.
- [5] W. Szpankowski, "Stability Conditions for Some Multiqueue Distributed Systems: Buffered Random Access Systems," *Adv. Appl. Probab.*, vol. 26, pp. 498–515, Jun. 1994.
- [6] W. Luo and A. Ephremides, "Stability of  $N$  Interacting Queues in Random-Access Systems," *IEEE Trans. Inf. Theory*, vol. 45, no. 5, pp. 1579–1587, Jul. 1999.
- [7] S. Ghez, S. Verdú, and S. C. Schwartz, "Stability Properties of Slotted Aloha With Multipacket Reception Capability," *IEEE Trans. Autom. Control*, vol. 33, no. 7, pp. 640–649, Jul. 1988.
- [8] V. Naware, G. Mergen, and L. Tong, "Stability and Delay of Finite-User Slotted ALOHA With Multipacket Reception," *IEEE Trans. Inf. Theory*, vol. 51, no. 7, pp. 2636–2656, Jul. 2005.
- [9] K.-H. Hui, W.-C. Lau, and O.-C. Yue, "Stability of Finite-User Slotted ALOHA under Partial Interference in Wireless Mesh Networks," in *PIMRC 2007*, Athens, Greece, Sep. 2007, to appear.
- [10] —, "Partial Interference and Its Relations to Traffic Engineering in Wireless Mesh Networks," *IEEE Trans. Wireless Commun.*, submitted to.
- [11] S. S. Lam, "Store-and-Forward Buffer Requirements in a Packet Switching Network," *IEEE Trans. Commun.*, vol. 24, no. 4, Apr. 1976.
- [12] R. M. Loynes, "The Stability of a Queue with Non-Independent Inter-arrival and Service Times," *Proc. Cambridge Phil. Soc.*, vol. 58, pp. 494–520, 1962.
- [13] J. R. Wieland, R. Pasupathy, and B. W. Schmeiser, "Queueing-Network Stability: Simulation-Based Checking," in *Proceedings of the 2003 Winter Simulation Conference*, vol. 1, Dec. 2003, pp. 520–527.
- [14] D. Kincaid and W. Cheney, *Numerical Analysis: Mathematics of Scientific Computing*, 3rd ed. Brooks/Cole, 2002.
- [15] J.-S. Chang and C.-K. Yap, "A Polynomial Solution for Potato-Peeling and Other Polygon Inclusion and Enclosure Problems," in *25th Annual Symposium on Foundations of Computer Science*, Oct. 1984, pp. 408–416.

**Ka-Hung Hui**

PLACE  
PHOTO  
HERE

**On-Ching Yue**

PLACE  
PHOTO  
HERE

**Wing-Cheong Lau**

PLACE  
PHOTO  
HERE